

Received 13 January 2025, accepted 27 January 2025, date of publication 4 February 2025, date of current version 11 February 2025.

Digital Object Identifier 10.1109/ACCESS.2025.3538628

RESEARCH ARTICLE

Island Partition Strategy Based on Entropy Method-Set Pair Analysis for Microgrids

ZHAOYANG ZHANG¹, HONG ZHANG¹, LI ZHOU¹, ZHIWEI LI¹, WEI WANG¹, SIHU CHU²,
WENHANG CHANG³, CAN WANG³, (Member, IEEE),
ZHUOLI ZHAO⁴, (Senior Member, IEEE), CHUN SING LAI⁵, (Senior Member, IEEE),
AND LOI LEI LAI⁴, (Life Fellow, IEEE)

¹State Grid Hubei Economic Research Institute, Wuhan 430077, China

²Hunan Electric Power Design Institute Company Ltd., Changsha 410007, China

³College of Electrical Engineering and New Energy, China Three Gorges University, Yichang 443002, China

⁴Department of Electrical Engineering, School of Automation, Guangdong University of Technology, Guangzhou 510006, China

⁵Department of Electronic and Electrical Engineering, Brunel University London, UB8 3PH London, U.K.

Corresponding author: Can Wang (xfcancan@163.com)

This work was supported by the National Natural Science Foundation of China under Grant 52107108.

ABSTRACT The scientific and reasonable island partition of microgrids containing DG is of great practical significance for ensuring the safe switching of microgrid island operation and improving the reliability of microgrid power supply. The existing island partitioning strategies focus on power balance and basic load distribution but often neglect multiple load attributes, resulting in failure to guarantee the reliability of the load power supply with a relatively high comprehensive evaluation level. Therefore, to comprehensively consider the influence of multiple load attributes on islanding, an island partitioning strategy based on entropy method-set pair analysis is proposed for microgrids in this paper. First, the entropy method is used to objectively assign the weights of three indexes of the level of the load, the economic loss of the load power outage and the coefficient of change per unit power. Next, the set pair analysis (SPA) principle is combined with the comprehensive connection degree of the index to determine the comprehensive connection degree of different loads while considering each index, and the connection degree is used as the final island partition power supply recovery coefficient of the load. Finally, the dynamic programming algorithm is used to solve the objective function of island partitioning. The IEEE-69 node system verifies the proposed strategy. The verification results show that compared with the existing methods, the proposed strategy can restore the power supply of the important load more effectively and reduce the economic loss when the load is cut off. The proposed island partitioning strategy shows significant potential in improving the reliability and economy of the power supply for microgrids with important loads, especially for microgrids with complex loads.

INDEX TERMS Entropy method, island partition, microgrid, set pair analysis.

I. INTRODUCTION

With the widespread integration of distributed generation (DG), particularly intermittent renewable energy sources such as wind and solar power, microgrids have emerged as small-scale power systems with self-management capabilities, playing a crucial role in ensuring power system stability and supply continuity. A microgrid typically consists

of distributed energy sources, energy storage systems, and controllable loads, and it can flexibly operate in both grid-connected and islanded modes [1]. In the grid-connected mode, the microgrid and the main grid work together. In island mode, the microgrid can operate independently when disconnected from the main grid, ensuring a continuous power supply to critical loads. To ensure the stability of the system under different operation modes, the operation control of the microgrid needs to achieve key objectives such as power sharing, voltage regulation, and energy balance [2].

The associate editor coordinating the review of this manuscript and approving it for publication was Yonghao Gui¹.

Island operation is an important operation mode for power grids to ensure the power supply of important loads in microgrids after a failure [3], [4]. Therefore, the scientific and reasonable island partition of microgrids containing distributed generation (DG) is of great practical significance for ensuring the safe switching of microgrid island operation, improving the reliability of the microgrid power supply, and reducing the loss of load power outages caused by power system failures [5], [6]. The IEEE Std.1547.4-2011 standard provides clear requirements for the design and operation of islanded power grids. It also supports the safe and stable operation of islanded microgrids through technical means [7]. In island partition for microgrids, the network structure must first be divided and then a reasonable island partition path must be found under the electrical and topological constraints of the island.

As a prerequisite for island operation, island detection is a critical step to ensure that microgrids can be separated from the main grid and enter the island operation state in a timely and accurate manner. The effective island detection method can quickly detect the island state, trigger the corresponding island partitioning strategy, and ensure the continuous power supply of important loads. At present, islanding detection methods can be divided into remote methods and local methods [8]. The remote method can detect the signal state of the switch for island protection. This method has no detection limited area and has no impact on the system, but it is costly and difficult to realize. Local methods can be further divided into active methods, passive methods and mixed methods [9]. The active method is used to judge the island state by injecting disturbance signals into the system. Common methods include the active frequency drift method (AFD) and impedance measurement method (IM) [10]. The passive method determines the island state by monitoring the natural variation in the system's electrical volume, such as voltage and frequency. Representative methods include the over/under voltage detection method (O/UV) [11], the over/under frequency detection method (O/UF) and the frequency change rate method (ROCOF) [12]. Combining the characteristics of the active method and passive method, the hybrid method can achieve higher detection accuracy and reliability, especially for complex systems, including the voltage fluctuation injection method [13], mixed slip mode frequency shift (SMS), and ROCOF method [14]. In recent years, islanding detection methods based on intelligent algorithms have shown significant advantages in improving detection accuracy and addressing complex scenarios. An anti-islanding protection scheme based on a support vector machine (SVM) is proposed in [15], where electrical parameters from the point of common coupling (PCC) are passively monitored, and an SVM is used for classification to determine whether an islanding event has occurred. A method for islanding detection based on convolutional neural networks (CNNs) is presented in [16], where time series data is transformed into images, and a CNN is employed to train and classify the data to identify islanding states. A fast islanding detection method

based on long short-term memory (LSTM) networks is introduced in [17], where a discrete Fourier transform (DFT) is applied to extract the symmetrical components of voltage and current signals, which are then classified via an LSTM classifier for efficient detection. These detection methods provide a fundamental basis for the successful implementation of island partitioning strategies.

Island partition can be categorized into intentional islanding and unintentional islanding according to differences in the partition method [18], [19]. Intentional islanding has an island area according to the capacity of DG in microgrids and the power of the load in microgrids and an island range that determines in advance in response to possible power failures in the system. Unintentional islanding refers to the state in which a microgrid unexpectedly separates from the main grid without prior planning or control, and continues to supply power to a local area. Intentional islanding can still ensure the stable operation of a small system of microgrids when microgrids are disconnected from the large grid. Microgrids in this mode have a relatively stable operation capability and can improve the black start capability of the system. A dynamically modified island partition strategy is proposed in [20]. This strategy simplifies the calculation process by not considering the controllability of the load when forming the primary island and then determines the final island area by modifying the primary island. In [21], an automated radial island partition strategy is proposed to address the uncertainty of power generation and load; this strategy formulates different island partition scenarios using the correlation between load and DG. An island partitioning strategy based on energy balance is proposed in [22], where energy indicators are defined to comprehensively consider the load demand and the power supply capability of distributed generation. The strategy divides the islanded regions under energy constraints. However, this research focuses on the economics of system operation after island partition and does not consider the load priority. To maintain the radiation characteristics of the island, an ear decomposition-based method island partition model is proposed in [23]; this is an elastic island model that can resist local disturbances and power mismatch. A directed graph-based island partitioning strategy is presented in [24], which introduces "virtual nodes" and "virtual demand" to construct a network model with branch direction flexibility. A two-stage "search and tune" strategy to allocate DG and optimize island partitioning is proposed in [25]; this strategy uses multiple tree knapsack problems (TKPs) to isolate primary islands and solves TKPs based on a branch delimitation algorithm to obtain the final island partition result. A bilevel optimization strategy is constructed in [26] to solve the optimal island for minimizing the economic cost during failure recovery and reactivating the load with the most power. A multiperiod dynamic island partitioning strategy is proposed in [27], where an initial islanding division plan is obtained via the Dijkstra algorithm and controllable loads are integrated into the scheduling, resulting in a more flexible dynamic island partitioning model. This intentional island

is selected based on using the DG output and load capacity in the microgrid to determine the initial island partition area in advance. However, the actual island occurrence time may be unpredictable, and the actual situation causes a certain deviation in the intended island partition area, resulting in low utilization efficiency of DG or the inability to handle the continuous power supply of important loads in microgrids.

Unlike the intentional island, the unintentional island refers to the state in which the microgrid is unexpectedly separated from the main grid and continues to supply power to local areas without preplanning and control. Aiming to address island partitioning within unintentional islanding in microgrids, a two-stage structure optimization strategy for microgrids is proposed in [28]. This strategy uses the implicit enumeration method to search for the initial island solution and then verifies the interrupt value and calculates the reactive power compensation to determine the final island. The method in [29] is based on the depth-first search algorithm to find the optimal island in the power circle. This method reconstructs the network for faults at different locations in the microgrid to restore the power supply of the microgrid to the greatest extent. A multilevel constrained optimal island partition model based on the energy index is proposed in [22], which modifies the island partition model through the power dispatching process and sequential power flow. The second-order cone relaxation technique is used in [30] to transform the island partition problem into a mixed integer second-order cone programming model, which considers DG output regulation and capacitor bank reactive power compensation constraints when constructing the island partition model of microgrids. According to the operation characteristics of DG in [31], the binary combination variable particle swarm algorithm is used to carry out the global optimal search of the power distribution system, and the island obtained by isolation has certain frequency regulation and voltage regulation capabilities. A two-stage robust optimization island partition strategy is proposed in [32]. The strategy uses the elliptical uncertainty set to address the load forecasting error, which makes the island partition more stable and reliable in the case of load fluctuation and realizes the maximum load recovery. An island partition method based on an intelligent algorithm is proposed in [33]. This method uses a graph convolution network combined with an autoencoder to realize the efficient extraction and optimization of power grid topology and communication characteristics and ensures the real-time stability of island partitioning.

According to the above research, when the system fails, the microgrids can form an island by DG to continuously supply power to the load, and island partition is important for restoring the power supply of the system after the failure. However, choosing which load power supply to restore is also worth studying. The various properties of the load affect the reliability and economy of the system after the island partition. To improve the stability and reliability of the power supply, we should fully utilize the power supply capacity of DG and maximize the range of the load power supply to

reduce the economic loss caused by load power outages to the microgrids. This requires developing a scientific and reasonable island partition scheme for the microgrid. The main contributions of this paper are as follows, with the differences compared with the other methods shown in Table 1:

TABLE 1. Comparison of the contributions of this paper with those of the relevant literature.

Literature	Consider the multiple properties of the load	Consider load priorities	Reduce the economic loss of power failure	Improve the accuracy of the results	Complexity	System components studied
[28]				✓	low	DG, load
[29]				✓	low	DG, load
[22]				✓	low	DG, load
[30]		✓		✓	intermediate	DG, load
[31]		✓	✓	✓	intermediate	DG, load
[32]		✓	✓	✓	higher	DG, load
[33]		✓		✓	higher	DG, load
Proposed Strategy	✓	✓	✓	✓	intermediate	DG, load

1) A method for determining the comprehensive connection degree of the load index based on the set pair analysis (SPA) principle is proposed, which differs from the island partition strategy based on economic cost index optimization in [21] and [26]. The proposed strategy utilizes the SPA principle to optimize different load indexes and describes the relationship between different loads and evaluation levels through the comprehensive connection degree of the load index.

2) A microgrid island partition strategy based on entropy method-set pair analysis is proposed. It differs from the Island partition strategy in [30], which considers only the important dead load weights. The strategy proposed in this paper combines the load weight and SPA principle to construct an island partition optimization model. The island partition optimization model can isolate the load nodes in various ways and determine the optimal island area.

The remainder of the paper is organized as follows. Section II details the method of determining the comprehensive connection degree of the proposed load index. Section III introduces the island partition model. Section IV gives case study and explanations to results. Finally, Section V provides a conclusion of this paper.

II. METHOD OF DETERMINING THE COMPREHENSIVE CONNECTION DEGREE OF THE LOAD INDEX

There is a complex relationship between the multiple attributes of the load and the operation of the microgrid system. Furthermore, the multiple attribute index of the load has

different degrees of influence on the continuous power supply of important loads and the economic operation after island partition. In this paper, the comprehensive connection degree of the load is used to reflect the interaction between different attributes of the load and the influence of the island partition of the microgrid. The weight of the load index is obtained by the entropy method, and the comprehensive connection degree of the load is determined by integrating SPA.

A. CALCULATION OF LOAD WEIGHT BASED ON THE ENTROPY METHOD

The entropy method calculates the weight of each index according to the degree of difference between each index. This is an objective assignment method that can avoid the influence of subjective artificiality to a certain extent. This method uses a mathematical model to directly measure the value of the attribute parameters of the evaluation object itself, providing objectivity. Since the entropy method can evaluate the evaluation indexes of different dimensions in the evaluation, it is widely used in multiobjective decision-making problems [34]. In this section, the level of the load, the economic loss of the load power outage, and the coefficient of change per unit power are selected as the index in the load evaluation system. The entropy method is used to determine the various indexes that affect the load evaluation in the island partition. The specific evaluation process is as follows:

1) Determine the original evaluation matrix of the evaluation system according to the total number m of loads participating in the evaluation and the total number n of load evaluation indexes:

$$X_{ij} = \begin{bmatrix} x_{11} & x_{12} & \cdots & x_{1n} \\ x_{21} & x_{22} & \cdots & x_{2n} \\ \vdots & \vdots & \vdots & \vdots \\ x_{m1} & x_{m2} & \cdots & x_{mn} \end{bmatrix} \quad (1)$$

where X_{ij} is the j th index value of load i ; m is the total number of loads; and n represents the total number of indexes participating in the evaluation.

2) Since the dimensions of each evaluation index are different, the judgment matrix X_{ij} is normalized as follows:

$$y_{ij+} = \frac{x_{ij} - \min \{x_{1j}, \dots, x_{mj}\}}{\max \{x_{1j}, \dots, x_{mj}\} - \min \{x_{1j}, \dots, x_{mj}\}} \quad (2)$$

$$y_{ij-} = \frac{\max \{x_{1j}, \dots, x_{mj}\} - x_{ij}}{\max \{x_{1j}, \dots, x_{mj}\} - \min \{x_{1j}, \dots, x_{mj}\}} \quad (3)$$

where Y_{ij} is the normalized value of the load index and includes two normalized forms, Y_{ij+} and Y_{ij-} ; Y_{ij+} is the value of the j th index of load i after positive normalization, and Y_{ij-} is the value of the j th index of load i after negative normalization.

3) Calculate the index entropy value of the load:

$$E_j = -\frac{1}{\ln(m)} \times \sum_{i=1}^m (f_{ij} \times \ln f_{ij}) \quad (4)$$

$$f_{ij} = Y_{ij} / \sum_{i=1}^m Y_{ij} \quad (5)$$

where E_j is the entropy of the j th evaluation index and f_{ij} is the proportion of the j th index of load i to all evaluation indexes.

When $f_{ij} = 0$, $\ln f_{ij}$ in Equation (4) is meaningless, so f_{ij} must be corrected. The correction equation F_{ij} is as follows [35]:

$$F_{ij} = (1 + Y_{ij}) / \sum_{i=1}^m (1 + Y_{ij}) \quad (6)$$

4) Express the weights of the load index calculated from the corrected entropy value as follows [36]:

$$\omega_j = (1 - E_j) / \sum_{j=1}^n (1 - E_j) \quad (7)$$

where ω_j is the entropy weight of the j th evaluation index; $1 - E_j$ represents the utility value of the j th evaluation index.

B. SET PAIR ANALYSIS PRINCIPLE AND COMPREHENSIVE CONNECTION DEGREE DETERMINATION

SPA theory is an effective mathematical tool for handling deterministic and uncertain problems. It primarily addresses uncertainty, and the set pair and correlation degree are its core ideas [37]. SPA theory skillfully combines dialectical thinking and mathematical methods while acknowledging contradictory objectivity. A set pair consists of two sets with a certain relationship. It uses the degree of connection to quantitatively describe the information of things and reflects the connection and transformation relationship between the sums of the two sets through “identity, difference, and opposition” [38].

1) THE PRINCIPLE OF SET PAIR ANALYSIS

Two sets A and B with a degree of connection are used. The degree of connection is used to indicate their “identity, difference, and opposition” characteristics. The degree of connection is expressed as [39]:

$$\mu_{A-B} = a + bI + cJ \quad (8)$$

$$a + b + c = 1 \quad (9)$$

$$a = \frac{S}{N}, \quad b = \frac{F}{N}, \quad c = \frac{P}{N} \quad (10)$$

where μ_{A-B} is the degree of connection of pairs of sets composed of two sets; a , b , and c are the degree of identity, difference and opposition, respectively; and I and J are the difference coefficient and the opposition coefficient, respectively, where the value range of I is $[-1, 1]$. When I is -1 or 1 , it is deterministic, and when I is closer to 0 , the uncertainty of b is stronger. J is usually taken as -1 . N is the total number of features contained in the set pair; S , F , and P are the common characteristic number, opposite characteristic number and neither common nor opposite characteristic number of the two sets, respectively.

2) THE DETERMINATION OF THE COMPREHENSIVE CONNECTION DEGREE

Load evaluation involves multiple evaluation indexes, and each index has a different influence effect on the operation of microgrids after islanding. Therefore, it is necessary to compare the identity, difference, and opposition connection degree μ_{ijk} between the evaluation index j of each load i and the evaluation index standard corresponding to each evaluation level. μ_{ijk} is then used to calculate the comprehensive connection degree \bar{u}_{ik} of load i . In this paper, the evaluation criteria of load consist of five levels: I, II, III, IV, and V, where I. is the best and V. is the worst. $s_k(k = 1, 2, 3, 4, 5)$ is the limit value corresponding to each level, and each level corresponds to a limit interval, as shown in Table 2.

The connection degree is the primary aspect of load stability evaluation regarding island partition. According to the data characteristics of each index of the load, the connection function μ_k of each level is expressed differently for different index pointing types.

Equation (9) can be further extended to:

$$\mu_k = \mu_{A-B} = a_{ij} + b_{ij_1}I_1 + b_{ij_2}I_2 + \dots + b_{ij_m}I_m + c_{ij}J \tag{11}$$

where a_{ij} and c_{ij} are the degree of identity and opposition corresponding to the evaluation index j of load i respectively, and b_{ij_1} , b_{ij_2} , and b_{ij_m} are the degree of difference corresponding to the evaluation index j of the extended load i .

When calculating the single-index connection degree μ_{ijk} , the load i and the evaluation standard level k associated with the load evaluation index j are regarded as two sets that form a set pair. Then, the quantitative analysis of ‘‘identity, difference, and opposition’’ is performed on their proximity attribute.

For the smaller and better index, the single index connection degree μ_{ijk} of the evaluation index of load i is calculated as follows [40]:

$$\mu_{ijk} = \begin{cases} 1, (x_{ij} < s_1) \\ \frac{s_1 + s_2 - 2x_{ij}}{s_2 - s_1} + \frac{2x_{ij} - 2s_1}{s_2 - s_1}i_1, \\ (s_1 < x_{ij} \leq \frac{s_1 + s_2}{2}) \\ \frac{s_2 + s_3 - 2x_{ij}}{s_3 - s_1}i_1 + \frac{2x_{ij} - s_1 - s_2}{s_3 - s_1}i_2, \\ (\frac{s_1 + s_2}{2} < x_{ij} \leq \frac{s_2 + s_3}{2}) \\ \frac{s_3 + s_4 - 2x_{ij}}{s_4 - s_2}i_2 + \frac{2x_{ij} - s_1 - s_2}{s_4 - s_2}i_3, \\ (\frac{s_2 + s_3}{2} < x_{ij} \leq \frac{s_3 + s_4}{2}) \\ \frac{2s_4 - 2x_{ij}}{s_4 - s_3}i_3 + \frac{2x_{ij} - s_3 - s_4}{s_4 - s_3}j, \\ (\frac{s_3 + s_4}{2} < x_{ij} \leq s_4) \\ j, (x_{ij} \geq s_4) \end{cases} \tag{12}$$

TABLE 2. Rating correspondence table.

Level	I	II	III	IV	V
Rank standard value	85-100	70-85	50-70	30-50	0-30

For the larger and better index, the single index connection degree μ_{ijk} of the evaluation index of load i is calculated as follows:

$$\mu_{ijk} = \begin{cases} 1, \\ (x_{ij} \geq s_1) \\ \frac{2x_{ij} - s_1 - s_2}{s_2 - s_1} + \frac{2s_1 - 2x_{ij}}{s_2 - s_1}i_1, \\ (\frac{s_1 + s_2}{2} \leq x_{ij} < s_1) \\ \frac{2x_{ij} - s_2 - s_3}{s_3 - s_1}i_1 + \frac{s_1 + s_2 - 2x_{ij}}{s_3 - s_1}i_2, \\ (\frac{s_2 + s_3}{2} \leq x_{ij} < \frac{s_1 + s_2}{2}) \\ \frac{2x_{ij} - s_3 - s_4}{s_4 - s_2}i_2 + \frac{s_1 + s_2 - 2x_{ij}}{s_4 - s_2}i_3, \\ (\frac{s_3 + s_4}{2} \leq x_{ij} < \frac{s_2 + s_3}{2}) \\ \frac{2x_{ij} - 2s_4}{s_4 - s_3}i_3 + \frac{s_3 + s_4 - 2x_{ij}}{s_4 - s_3}j, \\ (s_4 \leq x_{ij} < \frac{s_3 + s_4}{2}) \\ j, \\ (x_{ij} < s_4) \end{cases} \tag{13}$$

where x_{ij} is the sampling value of evaluation index j regarding load i . If the sampling value x_{ij} is within the range of values required by the evaluation standard level k , the index contact degree $\mu_{ijk} = 1$. If x_{ij} is in an interval level, then $\mu_{ijk} = -1$. If x_{ij} is on an adjacent scale, then $\mu_{ijk} \in [-1, 1]$. The closer x_{ij} is to level k , the closer μ_{ijk} is to 1, and the closer x_{ij} is to the level separated from level k , the closer μ_{ijk} is to -1 .

Among the three load evaluation indexes selected in this paper, the load importance level and unit power variation coefficient are positive indexes; the larger the value is, the better the performance. The economic loss of load outage is a negative index; the smaller the value, the better the performance. Using the corresponding connection degree function, the connection degree of each index is calculated, and the entropy weight value of the index is then coupled into the set pair connection. The comprehensive connection degree \bar{u}_{ik} between load i and the evaluation standard level is calculated as:

$$\begin{aligned} \bar{u}_{ik} &= \sum_{j=1}^m \omega_j \mu_{ijk} \\ &= \sum_{j=1}^m \omega_j (a_{ij} + b_{ij_1}I_1 + b_{ij_2}I_2 + b_{ij_3}I_3 + c_{ij}J) \end{aligned} \tag{14}$$

where ω_j is the weight of evaluation index j calculated in Equation (14); \bar{u}_{ik} is the comprehensive connection degree of the evaluation index of load i , and $\bar{u}_{ik} \in [-1, 1]$. If a greater identity between load i and evaluation index level k indicates \bar{u}_{ik} is closer to 1, load i is more likely to belong to evaluation level k . Conversely, if a greater difference between load i and evaluation index level k indicates \bar{u}_{ik} is closer to -1 , load i is more likely to not belong to evaluation level k .

In this section, the corresponding load evaluation method is established by combining the SPA theory and the load evaluation system, and the load index and the load evaluation level constitute a set pair. To distinguish more accurately between the load index and the load evaluation level, the triangular fuzzy number is converted into the connection degree according to the isolated threshold interval. The connection degree is used to express the relationship between the load index and the load evaluation standard and to reflect the impact of load on ensuring the reliable power supply of important loads and the economic operation of the system in the island partition. In the load evaluation standard of island partitioning, priority is given to the optimal comprehensive evaluation level I of the load, and the comprehensive connection degree \bar{u}_{ik} of the load belonging to level I is used as the reference for constructing the island partitioning model.

III. ISLAND PARTITION MODEL

Island partitioning requires a set of feasible partition criteria based on the characteristics of power system faults and the topology of the power grid, accounting for a variety of factors. These guidelines are designed to ensure the safety, reliability and stability of the system operation, which can not only ensure the stable operation of islands but also minimize the loss of power outages, thus improving the power supply quality and user satisfaction.

A. PRINCIPLE OF ISLAND PARTITION

When microgrids operate on an island, distributed generation sources independently supply power to the loads within the system. The primary issue of the island partition problem is selecting a suitable splitting point in the microgrid. When the power system fails, the island is formed according to the island partition area, and the load in the system is supplied by DG during the island until the power system failure is resolved. Microgrids must follow certain principles during island partitioning [41]:

1) The principle of priority of important loads. Interrupting load power supply may cause certain economic losses and will impact personal safety in severe cases. The power supply of the level I loads should be prioritized, and as such power should be provided to the level II and III loads first when the DG capacity is sufficient.

2) The principle of maximum load. To improve the utilization rate of DG in the microgrid and reduce energy waste, therefore as much as possible load power supply should be maintained in the system during island partitioning to reduce load power loss.

3) The principle of radial operation of the power grid. According to the requirements of open-loop operation of microgrids, it is required to ensure the network has a radial structure during island partitioning to improve the stability and reliability of microgrid operation.

4) The principle of a low number of switching actions. During island partitioning, the partition scheme with as few switching operations as possible should be selected to reduce the action loss of the switching element and improve the operation timeliness of the system.

B. OPTIMAL OBJECTIVE FUNCTION OF ISLAND PARTITION

In this paper, the maximum amount of comprehensive recovery of the microgrid postfault load is used as the objective function of island partitioning:

$$\max \sum_{i=1}^n \bar{u}_{ik} P_{Li} x_i \quad (15)$$

where \bar{u}_{ik} is the comprehensive connection degree of the index of load node i calculated in Equation (15); P_{Li} is the active power of load node i ; and x_i is an integer variable. When $x_i = 1$, load i is isolated into islands, and when $x_i = 0$, load i is not isolated into islands.

In addition, to further optimize the system operation status after island partitioning, this paper considers real-time estimation of line impedance as an auxiliary means. The real-time variation of line impedance reflects the operating conditions inside the island and the electrical characteristics of the line, including important information such as the power flow direction and line connectivity. These pieces of information provide the key basis for power scheduling and resource optimization after island partitioning.

Specifically, real-time line impedance estimation can monitor the power flow inside an island, identify potential overload routes, and avoid local overload problems caused by high impedance. Moreover, real-time line impedance estimation can dynamically adjust the reactive power allocation, optimize voltage regulation strategies, and thus improve the accuracy of reactive power control. Therefore, real-time evaluation of line impedance can further enhance the stability and reliability of system operation in islanding mode.

C. CONSTRAINTS

The island partition problem involves seeking the optimal solution for the objective function while satisfying the given constraints. The objective function for island partitioning should meet the following constraints.

1) COMPREHENSIVE POWER QUALITY CONSTRAINTS

In islanded microgrids, power quality directly impacts the system's safety and stability. Therefore, by comprehensively considering system frequency deviation, voltage deviation, and harmonic distortion, a comprehensive power quality

constraint is established as follows:

$$\begin{cases} \Delta f \leq \Delta f_{\max} \\ \Delta U = \left| \frac{U_i - U_N}{U_N} \right| \times 100\% \leq \Delta U_{\max} \\ THD_i \leq THD_{\max} \end{cases} \quad (16)$$

where Δf is the system frequency offset; Δf_{\max} is the maximum allowable frequency offset, which refers to the national standard GB/T 15945-2008 for 0.2 Hz; ΔU is the voltage deviation; U_i is the actual operating voltage of the node; U_N is the nominal voltage of the system; ΔU_{\max} is the maximum allowable voltage deviation, which refers to the national standard GB/T 12325-2008 and accounts for 7% of the nominal voltage; THD_i is the total distortion rate of the voltage for the node; and THD_{\max} is the maximum allowable total distortion rate of the voltage, which refers to the national standard GB/T 14549-1993 for 4%.

2) POWER FLOW CONSTRAINT

In an isolated island microgrid, a power flow constraint can ensure the balance of the power supply and demand, the stability of the node voltage and current, and the stable operation of the system. The specific formula is as follows:

$$P_i(t) = U_i(t) \sum_{j=1}^n U_j(t) (G_{ij} \cos \delta_{ij}(t) + B_{ij} \sin \delta_{ij}(t)) \quad (17)$$

$$Q_i(t) = U_i(t) \sum_{j=1}^n U_j(t) (G_{ij} \sin \delta_{ij}(t) - B_{ij} \cos \delta_{ij}(t)) \quad (18)$$

where $P_i(t)$ and $Q_i(t)$ are the active power and reactive power of node i at time t respectively; $U_i(t)$ and $U_j(t)$ are the voltage amplitudes of nodes i and j respectively; G_{ij} and B_{ij} are the admittance of branch $i - j$; and $\delta_{ij}(t) = \delta_i - \delta_j$ is the voltage phase angle difference of nodes i and j .

3) POWER CONSTRAINT WITHIN THE ISLAND

During island partition, it should be ensured that the maximum active power supplied by distributed generation supply in the island is not lower than the load power and that the reactive power is used for local compensation, which is expressed as follows:

$$\sum_{i=1}^n P_{Gi} - \sum_{j=1}^k P_{Li} \geq 0 \quad (19)$$

$$\sum_{i=1}^n Q_{Gi} - \sum_{j=1}^k Q_{Li} \geq 0 \quad (20)$$

where $\sum_{i=1}^n P_{Gi}$ and $\sum_{i=1}^n Q_{Gi}$ represent the active power and reactive power capacity of all distributed generation (DG) within the island, respectively, and $\sum_{i=1}^k P_{Li}$ and $\sum_{i=1}^k Q_{Li}$ represent the active power and reactive power capacity of all loads within the island, respectively.

4) NODE VOLTAGE CONSTRAINT

The voltage on the bus cannot exceed this limit; a high voltage will overheat or damage the equipment. A low voltage will lead to switching and protection issue, which will cause unreliable system action and affect the network stability. The node voltage constraint is expressed as follows:

$$U_{i\min} \leq U_i \leq U_{i\max} \quad (21)$$

where U_i represents the voltage at node i , while $U_{i\min}$ and $U_{i\max}$ represent the minimum and maximum values of the voltage at node i , respectively.

5) LINE CURRENT CONSTRAINT

To ensure that protective actions are not falsely triggered during islanded operation, the currents flowing through transformers and lines should not exceed their rated currents. Otherwise, protective actions will disconnect the line and cause a power imbalance in the island.

$$I_{\max ij} < I_{Nij} \quad (22)$$

where $I_{\max ij}$ represents the maximum current flowing through the transformer and the line, while I_{Nij} represents the rated current of the transformer and the line.

6) ISLAND RADIATION OPERATION CONSTRAINT

$$g \in G \quad (23)$$

where g represents the network topology structure after fault recovery, while G represents the set of network radial structures.

D. SOLUTION PROCEDURE

Island partitioning is used to restore the power supply of important loads as much as possible, thereby avoiding system overload caused by excessive load. However, island partitioning involves multiple factors, including load demand, DG output, stability, system capacity, and other aspects. These factors interact with and constrain each other, making solving island partition models difficult. The dynamic programming algorithm can optimize the solution process because of its powerful information processing ability. The algorithm first decomposes complex problems into simpler subproblems for solution and then constructs the global optimal solution to the original problem via the solutions of these subproblems. To address this, a dynamic programming algorithm is employed in this paper to solve the island partition model of a microgrid. This algorithm can obtain reasonable results within a short period, thereby enhancing the efficiency and precision of microgrid island partitioning [42].

1) DYNAMIC PROGRAMMING ALGORITHM

The dynamic programming algorithm uses the optimization principle to transform the model into a multistage decision problem for solving. The basic process is as follows:

Assume that node i is a stage variable, where $i = 0, 1, 2, 3 \dots n$. When the first i nodes are divided into j islands, the maximum load recovery capacity $f(i, j)$ is the state variable, and the end node k of the previous island is the decision variable, where $k = 0, 1, 2, 3 \dots n$.

First, initialize the boundary conditions, determine the starting point of the recursion, and ensure that the algorithm can correctly compute and find the optimal solution.

$$\begin{cases} f(0, 0) = 0 \\ f(i, 0) = f(0, j) = -\infty \end{cases} \quad (24)$$

where $f(0, 0) = 0$ indicates that the load recovery amount is 0 when there is no node or island; $f(i, 0) = f(0, j) = -\infty$ indicates that the load recovery amount is invalid when there is no island or node.

Second, the state transition equation is set up. The state transition equation is used to represent how to construct the solution to a larger problem from the solutions to subproblems. Specifically, for each node i and number of islands j , consider making node i the end node of a new island, calculate the load recovery capacity of this new island, and then combine it with the previous state. The state transition equation can be expressed as [20]:

$$f(i, j) = \max_{0 \leq k < i} \left\{ f(k, j-1) + \sum_k^{i-1} u_k P_k \cdot x_k \right\} \quad (25)$$

where $f(k, j-1)$ is the optimal solution of the previous state, representing the maximum load recovery amount when the first k nodes are divided into $j-1$ islands; $\sum_k^{i-1} u_k P_k \cdot x_k$ indicates the load recovery amount of the new island formed from node k to node $i-1$; u_k is the comprehensive connectivity of node k ; and P_k is the active power of node k ; and x_k is an integer variable. When $x_k = 1$, it indicates that load k is divided on the island, and when $x_k = 0$, it indicates that load k is not divided on the island.

Third, on the basis of the state transition equation, the solutions to all the subproblems are calculated to obtain $f(n, m)$, where n is the total number of nodes, and m is the number of islands.

Finally, the solutions are used for all known subproblems, backtrack from the final state to the initial state to determine the final island partition scheme.

The dynamic programming solving process is shown in the figure below.

2) ISLAND PARTITION PROCESS

By solving the objective island partition function, a more scientific and efficient island partition scheme will be obtained in this paper, providing effective technical support and assurance for microgrid restoration. The island partition process is shown in Fig. 2, and the specific process for solving the island partition problem are as follows:

1) The whole network structure information, fault occurrence location, distributed generation (DG) outputs, and load

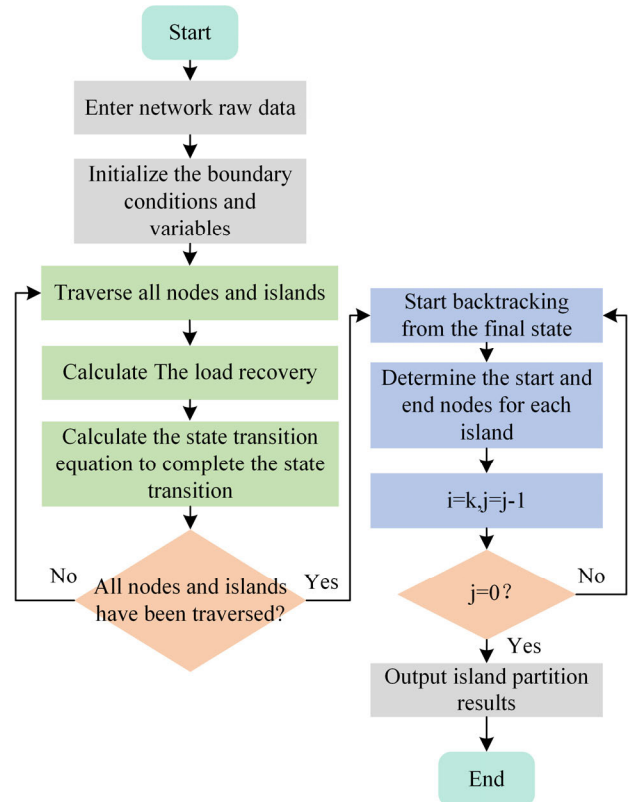


FIGURE 1. Solution flow of the dynamic programming algorithm.

capacity are read to initialize the state variables for the dynamic programming algorithm.

2) The entropy method is used to calculate the index weight evaluation level. Then, the entropy weight of the load evaluation index and the index connection degree are coupled into the comprehensive connection degree of the load evaluation index.

3) The dynamic programming algorithm is used to search and isolate the primary island range. After the partition, whether the important loads are all on the island is determined. If not, step 4) is completed; otherwise, step 5) is completed.

4) The dynamic programming algorithm is used again to traverse all nodes to ensure that all level I loads enter the island area to restore the power supply. The island area is then updated.

5) Whether the power balance constraint has been satisfied is determined. If not, some of the level II and III loads are removed to adjust the power supply area, and the island range is updated again until the power balance constraint is satisfied. The next step is then completed.

6) The final island partition result is obtained.

IV. CASE STUDY

A. PARAMETER SETTING

To validate the performance and feasibility of the island partitioning strategy proposed in this paper, the proposed island partitioning scheme, Scheme A, is compared with the island

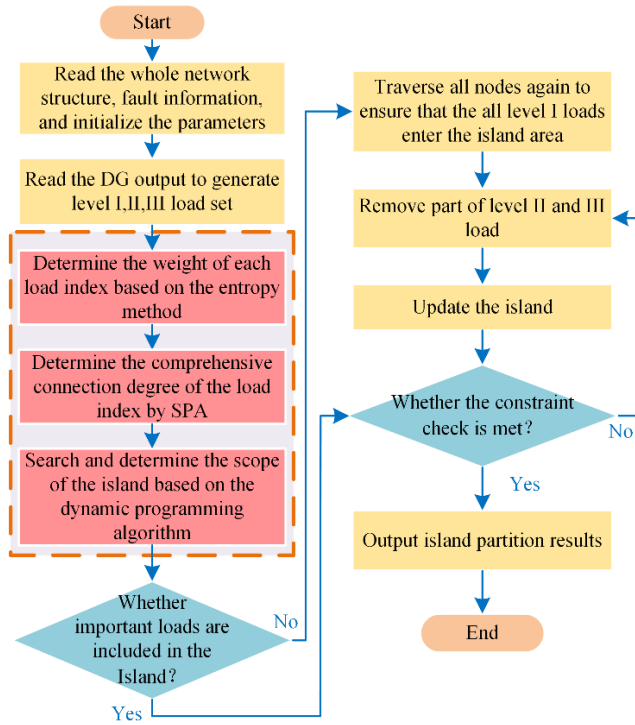


FIGURE 2. Island partition flow chart.

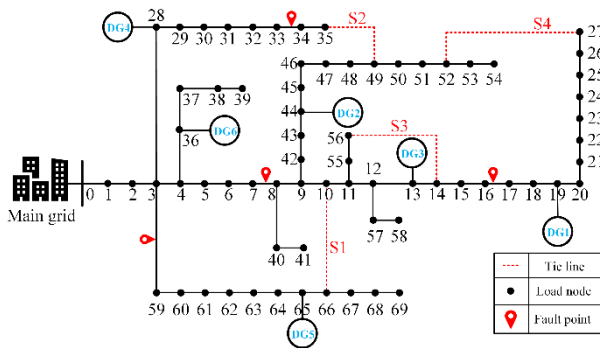


FIGURE 3. IEEE 69 node microgrid system.

TABLE 3. Distributed generation parameters.

Number	Installation node	Rated power/kW	Output power/kW
ing	locations		
DG1	19	550	370
DG2	44	230	100
DG3	13	140	250
DG4	28	210	100
DG5	65	850	250
DG6	36	210	55

partitioning Schemes B and C proposed in [26] and [30]. The differences in the island partitioning effect and quality of the three strategies are compared. DG is connected to the IEEE-69 node distribution system, and the load information of each

TABLE 4. Load level.

Load level	Load number
Level I loads	6,9,12,15,18,32,42,57,62,67
Level II loads	others
Level III loads	7,10,11,13,16,22,28,43,45,46,47,48,59,60,63

node provided in [31] is analyzed. The microgrid is located at the end of the main grid, and island partitioning is carried out within the microgrid. The microgrid connected with six DGs is shown in Fig. 3, where the solid line represents the branch connected with the segmented switch, and the virtual line is the tie line branch connected with the tie switch. The six distributed power parameters and their installation nodes in the system are shown in Table 3. The priority level of load importance is shown in Table 4. The level I load has the highest importance, the level III load has the lowest importance, and the level II load is between the two. In grid-connected operation, the DG uses PQ control to regulate active and reactive power output, relying on the main grid for voltage and frequency references. In islanded operation, a leader-follower control strategy is adopted, with the gas turbines (GTs) acting as the leader source via V/f control to provide voltage and frequency references for the photovoltaics (PVs) and wind turbines (WTs). The PVs and WT, as follower sources, continue to use PQ control. In this experimental test scenario, it is assumed that four permanent faults occur in the microgrid at the same time, and the fault lines have been disconnected from the other branches of the microgrid. The fault lines are 7-8, 16-17, 3-9 and 33-34.

B. COMPARISON ANALYSIS OF ISLAND PARTITION WITHOUT CONSIDERING TIE LINE SWITCHES

This section discusses island partition scenarios when contact switches S1, S2, S3, and S4 are disconnected in the system. In these scenarios, the superior power grid fails, the line node 0-1 is disconnected, and four faults occur in the microgrid. The power shortage area of the microgrid operates in an island mode, and the load power supply is maintained through the distributed power output in the system. The island partition results of each scheme are shown in Fig. 4.

The island partitioning result for the proposed Scheme A is shown in Fig. 4(a). The island partitioning result for Scheme B is shown in Fig. 4(b), and the island partitioning result for Scheme C is shown in Fig. 4(c). All three schemes divide the microgrid into five islanded areas: Island 1 contains DG4 and DG6, Island 2 contains DG2, Island 3 contains DG5, Island 4 contains DG3, and Island 5 contains DG1. Due to the different island partitioning basis of each scheme, there are some differences in the specific load partition for Islands 1, 2, and 4 among the three schemes.

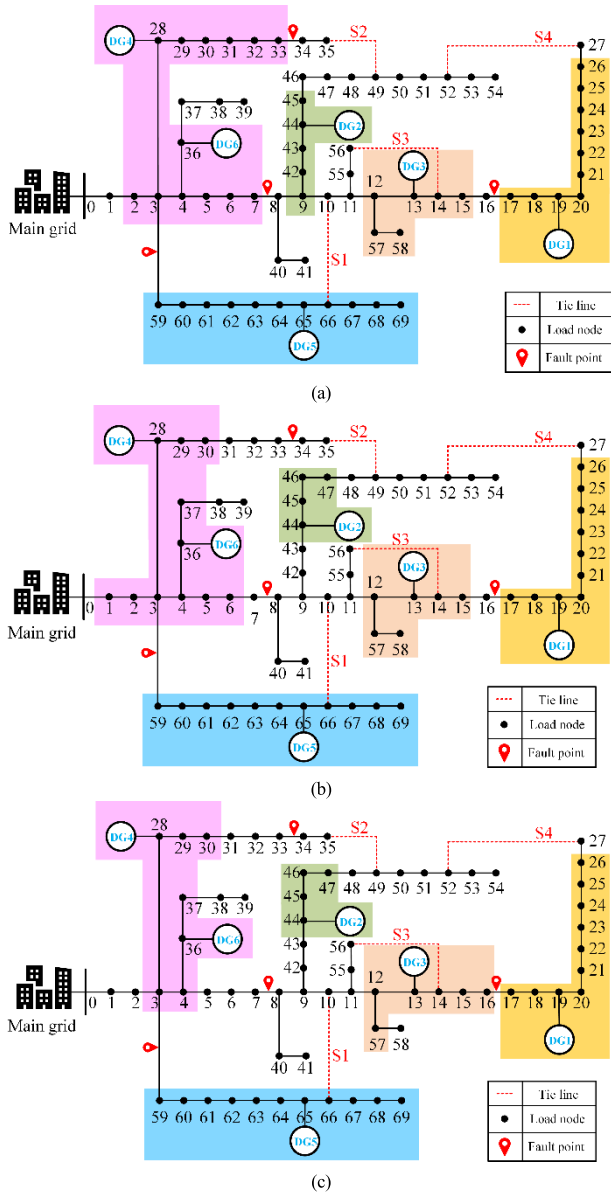


FIGURE 4. The island partition diagram of each strategy without considering the tie lines. (a) Illustration of the island partition for scheme A; (b) illustration of the island partition for scheme B; (c) illustration of the island partition for scheme C.

Fig. 5(a) represents the load distribution within each island for the proposed Scheme A in this scenario. This figure demonstrates that the level I load percentages within Islands 1-5 are 9.44%, 37.44%, 15.41%, 80.29%, and 16.84%, respectively. Fig. 5(b) shows the load distribution within each island for Scheme B. The proportion of level I load isolated in Islands 1-5 under this strategy is 0.17%, 0%, 15.41%, 77.47%, and 16.84%, respectively. Fig. 5(c) depicts the load distribution within each island in Scheme C. The proportion of level I load isolated in Islands 1-5 under this strategy is 0%, 0%, 15.41%, 71.84% and 16.84%, respectively. In forming islands, Scheme B and Scheme C have island areas without important loads. Table 5 presents a comparison of the island

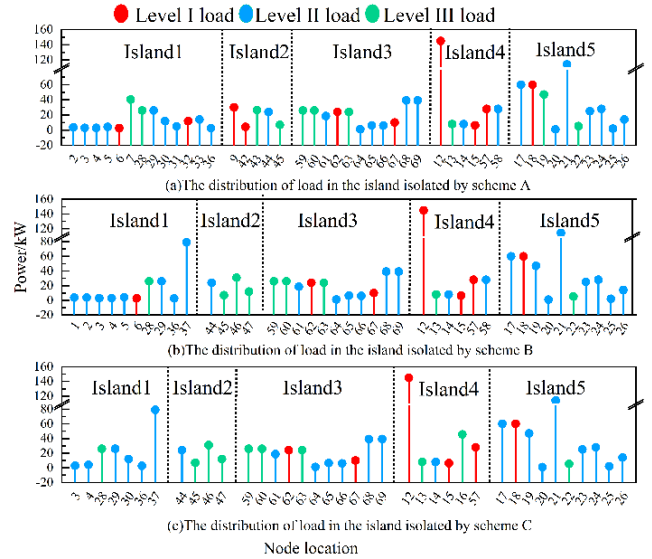


FIGURE 5. Load distribution on each Island for different schemes.

partitioning results for the three strategies. The comparison demonstrates that Scheme A achieves a level I load restoration power of 322.25 kW, with a level I load restoration rate of 100%. However, Scheme B and Scheme C achieve level I load restoration powers of 269.6 kW and 267 kW with level I load restoration rates of 83.66% and 82.85%, respectively. Because Scheme B does not consider the level of importance for the load when isolating, it fails to ensure that all level I loads are restored to the power supply. Although Scheme C considers the load importance, this method fixes the weight of the load level when addressing the island partition optimization problem, taking it as a single weight coefficient. The target optimization product is overly large when the scheme is faced with large power level II and level III loads, which leads to the strategy misjudging the level I load. Therefore, the recovery of the level I load under Scheme C is incomplete. In the process of load evaluation, Scheme A fully considers the importance level of the load. In island partitioning, this scheme assigns different weights to the influence of different attributes of the load, which optimizes the disadvantages of fixed weights in the solution. Therefore, during an island partitioning, the load I in the system is isolated into a continuous power supply in the island. The economic loss of power outage per unit time caused by the island formed after the partition of Scheme A is \$44.88/kWh, while the economic loss of power outage per unit time caused by the island formed after the partition of Scheme B and Scheme C are \$53.19/kWh and \$53.62/kWh, respectively. Because Scheme A fully considers the economic loss of power outage when dividing the load, it prioritizes by dividing the load with greater economic loss of power outage into power supply in the island and decreasing the economic loss of the whole system. Scheme B considers the economic cost of the whole island partition system. It does not specifically consider for the power outage loss caused by the level I load when dividing

TABLE 5. Comparison of Island partition strategies results.

Island Strategies	Scheme A	Scheme B	Scheme C
Recovery rate of level I load	100%	83.66%	82.85%
Economic loss due to power outage per unit time (\$/kWh)	44.88	53.19	53.62
Number of loads supplied with power	45	41	38
Number of switching actions	8	8	9
DG utilization rate	93.04%	91.39%	92.75%

the load, resulting in a higher economic loss than that caused by Scheme A. Scheme C does include the outage loss of the load, so the economic loss under this strategy is the largest. At the same time, the number of load power supply nodes in the island partition given by the proposed strategy is 4 and 7 more than that of Scheme B and Scheme C, respectively. This is because Scheme A abandons the nodes 37, 46 and 16 with larger power in the island partition and includes more nodes with smaller power in the island range. In addition, while forming island 4, Scheme A abandons the power supply of level III load node 16 and supplies power to level II load node 58, to ensure the continuous power supply to more high priority loads. Although the DG utilization rate in island 4 is lower than that in island 4 isolated by Scheme C, the DG utilization rate in the whole island system isolated by Scheme A is still the highest of the three schemes. Compared with Schemes B and C, Scheme A can fully consider the influence of each index on the load when using the comprehensive connection degree to select the load. During island partitioning, it can ensure the continuous power supply of important loads and reduce the economic loss of power outages. Scheme A also optimizes the power distribution and voltage regulation within the island by estimating the line impedance in real-time, ensuring a stable power supply of critical loads in island mode. In addition, this method also improves the utilization efficiency of DG in islanded microgrids.

C. COMPARATIVE ANALYSIS OF ISLAND PARTITION CONSIDERING TIE-LINE SWITCHING

To further verify the superiority of the proposed strategy in island partitioning, the three schemes described in Section B are further compared in this section. The actions of the system tie line switches S1, S2, S3, and S4 are considered in this case test. In this scenario, the upper power grid fails, the line node 0-1 is disconnected, and four permanent faults occur in the microgrid. The island partition of the three schemes described in Section IV-B is shown in Fig. 5. Fig. 6(a) depicts the four islanded areas formed by Scheme A. Island 1 contains DG4 and DG6. Island 2 contains DG2 and DG5, and it closes the interconnecting line switch S1. Island 3 contains DG3, and it closes the interconnecting line switch S3. Island 4 contains DG1, and it closes the interconnecting line switch S4.

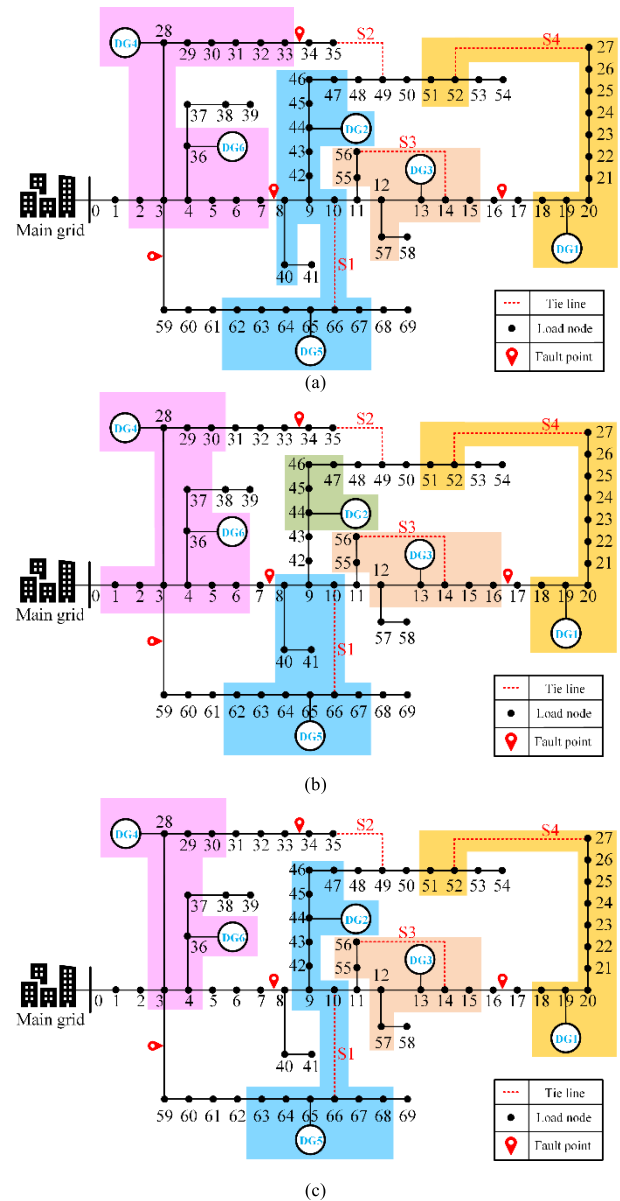


FIGURE 6. Island partition diagram for each strategy considering the tie line. (a) Illustration of Island partition in scheme A; (b) Illustration of Island partition in scheme B; (c) Illustration of Island partition in scheme C.

Fig. 6(b) depicts the five islanded areas formed by Scheme B. Island 1 contains DG4 and DG6. Island 2 contains DG2. Island 3 contains DG5, and it closes the interconnecting line switch S1. Island 4 contains DG3, and it closes the interconnecting line switch S3. Island 5 contains DG1, and it closes the interconnecting line switch S4. Fig. 6(c) depicts the four islanded areas formed by Scheme C. Island 1 contains DG4 and DG6. Island 2 contains DG2 and DG5, and it closes the interconnecting line switch S1. Island 3 contains DG3, and it closes tie line switch S3. Island 4 contains DG1, and it closes tie line switch S4.

Fig. 7(a) depicts the load distribution within each island for the proposed Scheme A in this event. The figure demonstrates

that the percentages of level I loads within Islands 1-4 are 9.44%, 19.54%, 77.52%, and 16.65%, respectively. Fig. 7(b) illustrates the load distribution within each island for Scheme B. Under this strategy, the percentages of level I loads within Islands 1-5 are 1.68%, 0%, 25.73%, 60.81%, and 16.65%, respectively. Fig. 7(c) presents the load distribution within each island for Scheme C. Under this strategy, the percentage of level I loads within Islands 1-4 is 0%, 12.69%, 77.52%, and 16.65%, respectively. When considering the closure of the tie line switch, some island areas within the island ranges isolated by Scheme B and Scheme C still do not contain level I loads. In this scenario, Scheme A ensures the reliable power supply of level I loads in each island area.

The comparison of the results after partitioning under the three schemes is shown in Table 6. The comparison demonstrates that Scheme A has a level I load restoration power of 322.25 kW, with a level I load restoration rate of 100%. However, Scheme B and Scheme C have level I load restoration powers of 277.9 kW and 283.65 kW, with level I load restoration rates of 86.24% and 88.02%, respectively. Because Scheme B does not consider the importance level of the load when dividing, it fails to ensure that all level I loads are restored to the power supply. Scheme C is limited by the influence of the fixed load weight, which leads to misjudgment of the important load, so the recovery of the level I load under Scheme C is incomplete. However, Scheme A optimizes the fixed weight disadvantage in the solution, so it divides the level I load in the system into a continuous power supply on the island during island partitioning. At the same time, the recovery rates of level I loads of Schemes A, B and C in this scenario are better than those obtained when the tie line switch is closed. The unit time economic loss due to power outage caused by the island partition for the three schemes A, B, and C is 39.94 \$/kWh, 45.31 \$/kWh, and 47.86 \$/kWh, respectively. Since Scheme A fully considers the economic loss of the load power outage during island partitioning, it fully prioritizes restoring the load with a large power outage loss in the process of load selection while forming the island, minimizing the load power outage loss of the island operation. Scheme B considers the total economic cost in the recovery process after island partitioning, and Scheme C does not consider the economic loss of island operation. As a result, Scheme B and Scheme C ignoring the economic loss caused by load outages in the process of load selection. At the same time, Scheme B does not consider the importance level of the load, and removing important loads causes economic loss to the whole system. In addition, Scheme A closes the tie line switches S1, S3, and S4, abandons the load nodes such as 68, 69, and 17 with large power, and accesses small load nodes to restore more load power supply and increase the power supply area under limited DG output power. The island isolated by Scheme A fully utilizes the output power of DG. The DG utilization rate of the island in Scheme A is 97.43%, while the DG utilization rates of the islands in Schemes B and C are 96.56% and 97.14%, respectively. In the scenario where the tie line switch is closed, each scheme

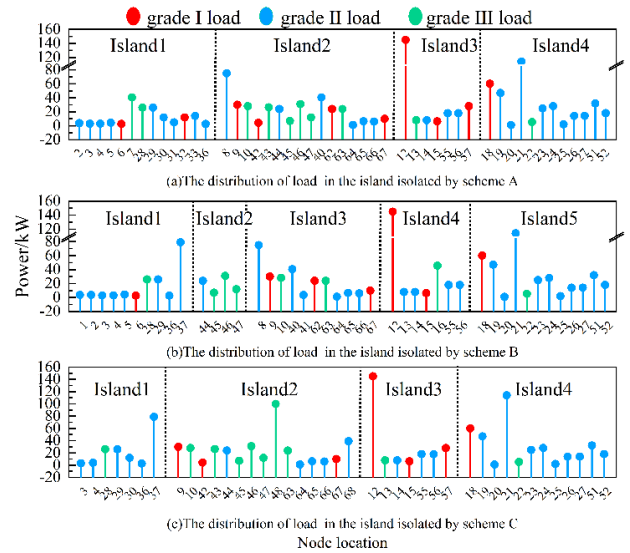


FIGURE 7. Load distribution within the island for each scheme.

TABLE 6. Comparison of Island partition strategy results.

Island Strategy	Scheme A	Scheme B	Scheme C
Recovery rate of level I load	100%	86.24%	88.02%
Economic loss due to power outage per unit time (\$/kWh)	39.94	45.31	47.86
Number of loads supplied with power	48	45	41
Number of switch actions	17	17	19
DG utilization rate	97.43%	96.56%	97.14%

effectively improves the utilization rate of DG in the island and restores the load power supply in the island as much as possible. Scheme A recovers more load power supply in the island partition, reducing the loss caused by the load when the power is cut off. Scheme A optimizes the power regulation and power distribution within the island through real-time estimation of line impedance, thereby improving system stability. This scenario test again verifies that the proposed scheme can ensure the continuous power supply of important loads compared with Scheme B and Scheme C in the island partition. It can also reduce the economic loss in the island partition and improve the utilization efficiency of DG in the microgrid.

D. COMPARATIVE ANALYSIS OF ISLAND PARTITION CONSIDERING THE UNCERTAINTY OF DISTRIBUTED GENERATION OUTPUT

The types of DGs used in this paper include GTs, PVs, and WTs. The output power is affected by time and weather conditions. Specifically, during the day, photovoltaic plants can provide ample power output, whereas at night, with no solar radiation, the output power of photovoltaic plants is

TABLE 7. Distributed power average power settings.

Numbering	Installation node locations	Average daytime power/kW	Average nighttime power/kW	Types of DG
DG1	19	550	550	GT
DG2	44	230	230	GT
DG3	13	200	0	PV
DG4	28	150	0	PV
DG5	65	600	650	WT
DG6	36	210	250	WT

TABLE 8. Comparison of Island partition strategies results.

Isolated condition	Daytime	Nighttime
Recovery rate of level I load	100%	100%
Economic loss due to power outage per unit time (\$/kWh)	41.32	44.65
Number of loads supplied with power	49	46
Number of switching actions	8	8
DG utilization rate	94.112%	90.856%

TABLE 9. Setting of coefficients of difference degrees and opposition degrees.

Test number	Difference coefficient	Opposition coefficient
	I	J
a	1	-1
b	0.5	-1
c	0	-1
d	-0.5	-1
e	-1	-1

TABLE 10. Comparison of Island partition strategies results.

Isolated condition	Test a	Test b	Test c	Test d	Test e
Recovery rate of level I load	100%	100%	100%	100%	100%
Economic loss due to power outage per unit time (\$/kWh)	40.01	41.21	42.73	41.36	40.22
Number of loads supplied with power	47	42	40	42	47
Number of switching actions	8	8	9	8	8
DG utilization rate	93.426%	92.329%	91.854%	92.272%	93.345%

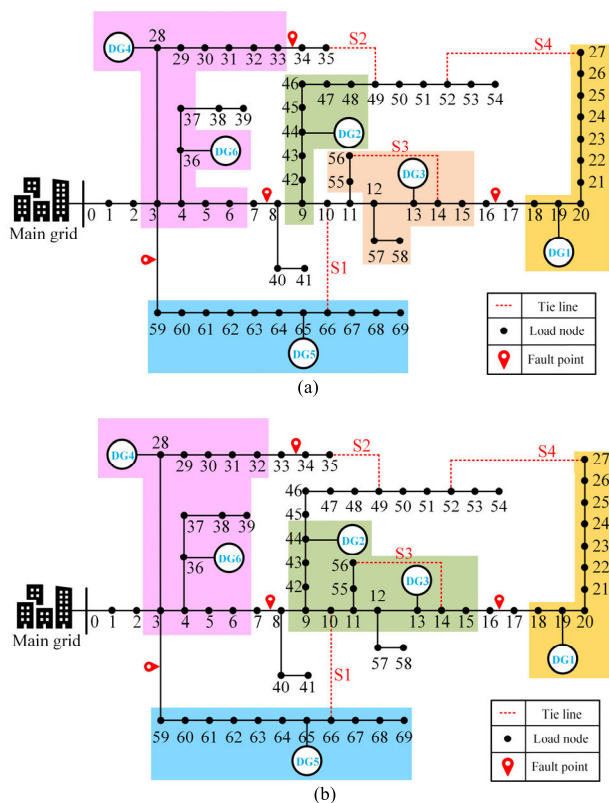


FIGURE 8. Island partition diagrams of Scheme A at different periods. (a) Diagram of the daytime island partition; (b) Diagram of the nighttime island partition.

zero. Moreover, the wind power output is greater at night than during the day, and the output power of the GT remains stable both during the day and at night. The average power of the distributed sources during the day and night is shown in Table 7.

To verify the impact of the uncertainty in the DG output on the island partition strategy proposed in this paper, a comparative analysis of the island partition results for day and night is conducted without considering tie line switches. Suppose that a fault occurs in the superior power grid, causing line nodes 0-1 to disconnect, and four additional faults occur within the microgrid. The island partition results for the daytime are

shown in Figure 8(a), and the results for the nighttime are shown in Figure 8(b). During the day, the system is divided into five islanded areas, whereas at night, it is divided into four islanded areas.

The comparison of the island partition results for daytime and nighttime is shown in Table 8. The comparison results indicate that, under different operating conditions during the day and night, the island partition strategy proposed in this paper can ensure the complete restoration of the level I load, from \$41.32/kWh during the day to \$44.65/kWh at night due decreases from 49 to 46, these changes are relatively small, indicating the strong robustness of the strategy.

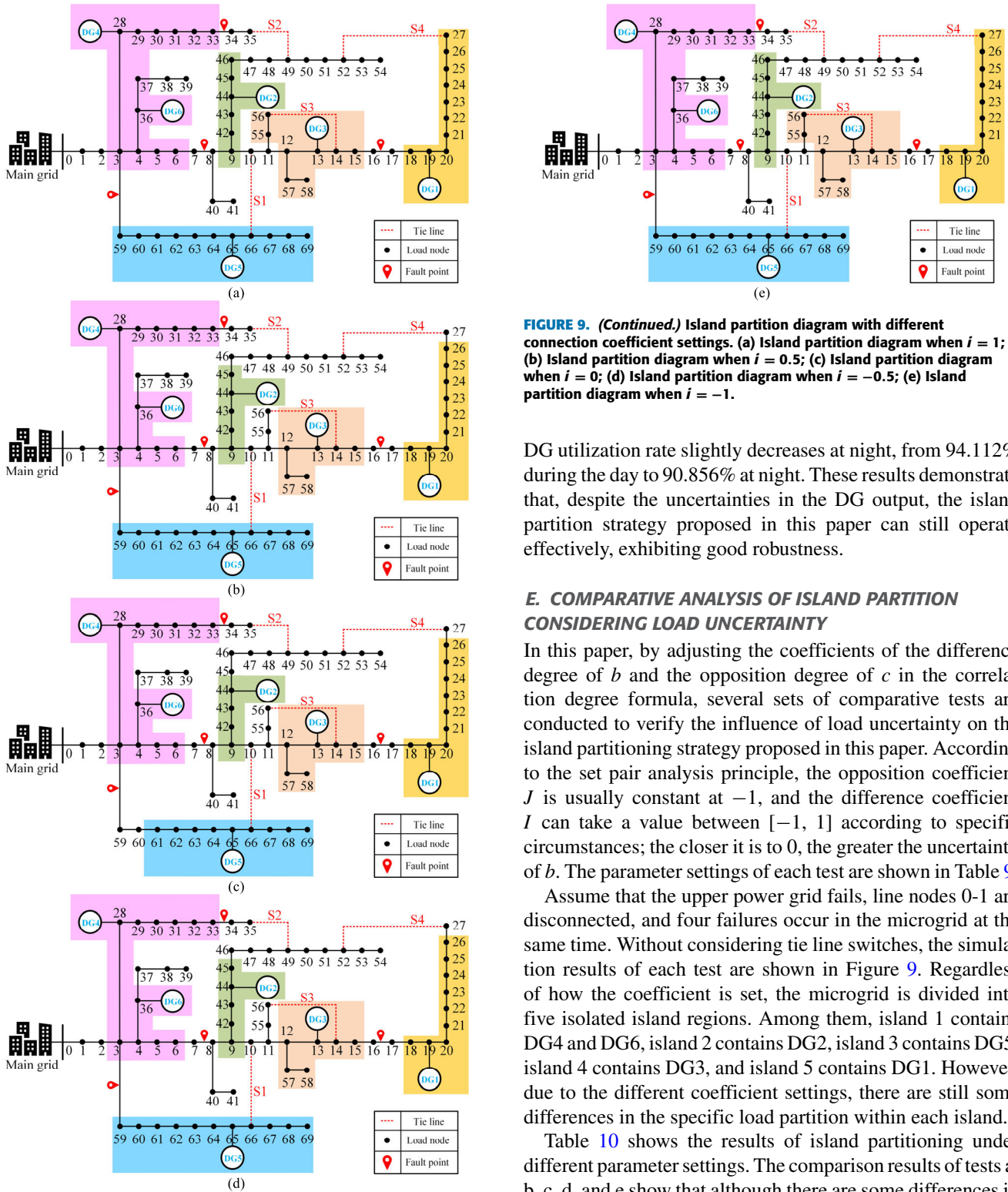


FIGURE 9. Island partition diagram with different connection coefficient settings. (a) Island partition diagram when $i = 1$; (b) Island partition diagram when $i = 0.5$; (c) Island partition diagram when $i = 0$; (d) Island partition diagram when $i = -0.5$; (e) Island partition diagram when $i = -1$.

Additionally, the number of switching operations remains constant at 8 times both during the day and at night, and the

FIGURE 9. (Continued.) Island partition diagram with different connection coefficient settings. (a) Island partition diagram when $i = 1$; (b) Island partition diagram when $i = 0.5$; (c) Island partition diagram when $i = 0$; (d) Island partition diagram when $i = -0.5$; (e) Island partition diagram when $i = -1$.

DG utilization rate slightly decreases at night, from 94.112% during the day to 90.856% at night. These results demonstrate that, despite the uncertainties in the DG output, the island partitioning strategy proposed in this paper can still operate effectively, exhibiting good robustness.

E. COMPARATIVE ANALYSIS OF ISLAND PARTITION CONSIDERING LOAD UNCERTAINTY

In this paper, by adjusting the coefficients of the difference degree of b and the opposition degree of c in the correlation degree formula, several sets of comparative tests are conducted to verify the influence of load uncertainty on the island partitioning strategy proposed in this paper. According to the set pair analysis principle, the opposition coefficient J is usually constant at -1 , and the difference coefficient I can take a value between $[-1, 1]$ according to specific circumstances; the closer it is to 0, the greater the uncertainty of b . The parameter settings of each test are shown in Table 9.

Assume that the upper power grid fails, line nodes 0-1 are disconnected, and four failures occur in the microgrid at the same time. Without considering tie line switches, the simulation results of each test are shown in Figure 9. Regardless of how the coefficient is set, the microgrid is divided into five isolated island regions. Among them, island 1 contains DG4 and DG6, island 2 contains DG2, island 3 contains DG5, island 4 contains DG3, and island 5 contains DG1. However, due to the different coefficient settings, there are still some differences in the specific load partition within each island.

Table 10 shows the results of island partitioning under different parameter settings. The comparison results of tests a, b, c, d, and e show that although there are some differences in the economic loss of power outage per unit time, the number of loads supplied with power, and the utilization rate of DGs, the overall performance is not different. The recovery rate of the level I load in all the tests is 100%, and the number of switch actions is almost the same. This shows that the island partition strategy proposed in this paper can effectively cope with load uncertainty and has good robustness and stability.

TABLE 11. Load power and economic loss due to power outage per unit time.

Load number	Power(kW)	Economic loss due to power outage per unit time (\$/kWh)
1	4.23	0.84
2	3.66	0.22
3	3	0.79
4	3	0.47
5	4.3	0.35
6	2.6	1.03
7	40.4	0.68
8	75	0.57
9	30	2.64
10	28	1.01
11	145	2.34
12	145	3.05
13	8	1.06
14	8	1.18
15	6.3	2.36
16	45.5	1.34
17	60	1.77
18	60	2.42
19	47	1.66
20	1	0.55
21	114	2.12
22	5.3	1.56
23	25	1.84
24	28	2.14
25	2	2.56
26	14	1.86
27	14	1.63
28	26	2.25
29	26	2.34
30	12	1.56
31	5	1.75
32	12	2.44
33	14	2.13
34	19.5	2.05
35	6	1.98

TABLE 11. (Continued.) Load power and economic loss due to power outage per unit time.

36	2.7	1.58
37	79	2.36
38	384.7	1.84
39	384.7	1.84
40	40.5	2.55
41	3.6	2.16
42	4.35	1.36
43	26.4	1.12
44	24	2.05
45	7	1.03
46	31	1.16
47	12	1.01
48	100	2.32
49	26	1.32
50	1244	3.66
51	32	2.56
52	18	2.86
53	227	2.44
54	59	2.16
55	18	1.44
56	18	1.44
57	28	1.03
58	28	1.07
59	26	1.17
60	26	1.17
61	18.6	1.65
62	24	3.11
63	24	2.13
64	1.2	0.59
65	6.4	0.68
66	6	1.03
67	10	1.25
68	39.22	2.23
69	39.22	2.23

V. CONCLUSION

To address the difficulty of directly evaluating the multiple attributes of the load and the load data information, an island

partition strategy based on entropy method-set pair analysis is proposed in this paper. The proposed strategy directly uses the data information of the load itself through the entropy value to objectively evaluate the level of the load, the economic loss of the load outage and the unit power change

coefficient, fairly assigns different indicators, and determines the weight of different index attributes of the load in the overall evaluation through this method. Then, the SPA principle is used to describe the degree of fit between various indicators of different loads, and the connection degree is used for “same, different and reverse” quantitative analysis. The uncertainty factors and deterministic factors of load indicators are included in the comprehensive connection degree for dialectical analysis and mathematical processing. The test results show that the islanding strategy proposed in this paper reduces the economic loss caused by load outages and ensures the power supply reliability of important loads in the process of island partitioning because it fully evaluates the load priority and power outage economic loss.

However, the island partitioning method proposed in this paper has certain limitations. First, the method relies heavily on the accuracy of the load data. If these data are inaccurate or incomplete, the partitioning results may deviate, reducing the reliability of the approach. Second, the method is somewhat dependent on the microgrid’s network topology. If the grid structure undergoes significant changes, the partitioning strategy may need to be readjusted. Future research will focus on improving the robustness of the method against uncertainties in load data and developing more flexible island partitioning strategies to adapt to changes in grid topology.

APPENDIX

See Table 11.

REFERENCES

- [1] C. Wang, S. Chu, H. Yu, Y. Ying, and R. Chen, “Control strategy of unintentional islanding transition with high adaptability for three/single-phase hybrid multimicrogrids,” *Int. J. Electr. Power Energy Syst.*, vol. 136, Mar. 2022, Art. no. 107724.
- [2] Z. Zhao, J. Xie, J. Xu, L. Xi, S. Gong, J. Lu, Y. Zeng, Q. Ni, and L. L. Lai, “Assessment and mitigation of multi-mode oscillations in wind-solar hybrid multi-microgrids,” *IEEE Trans. Smart Grid*, vol. 15, no. 2, pp. 1330–1345, Mar. 2024.
- [3] C. Wang, M. Wang, A. Wang, X. Zhang, J. Zhang, H. Ma, N. Yang, Z. Zhao, C. S. Lai, and L. L. Lai, “Multiagent deep reinforcement learning-based cooperative optimal operation with strong scalability for residential microgrid clusters,” *Energy*, vol. 314, Jan. 2025, Art. no. 134165.
- [4] W. Fu, B. Zheng, S. Li, W. Liao, Y. Huang, and X. Chen, “Batch channel normalized-CWGAN with Swin transformer for imbalanced data fault diagnosis of rotating machinery,” *Meas. Sci. Technol.*, vol. 36, no. 1, Jan. 2025, Art. no. 016207.
- [5] Z. Zhao, J. Wu, X. Luo, J. Xie, Q. Yang, Q. Ni, and L. L. Lai, “Reduced-order model for wind-solar multi-microgrids considering time-scale coupling,” *IEEE Trans. Power Syst.*, vol. 39, no. 1, pp. 2052–2065, Jan. 2024.
- [6] H. Xu, J. Ma, F. Xue, X. Li, H. Li, W. Wang, Y. Zhong, J. Zhao, and Y. Zhang, “Optimization control strategy for photovoltaic/hydrogen system efficiency considering the startup process of alkaline electrolyzers,” *Int. J. Hydrogen Energy*, vol. 106, pp. 65–79, Mar. 2025.
- [7] W. Fu, Y. Gao, Y. Zhang, X. Tu, S. Hu, and Y. Huang, “A distributed time-varying inherent privacy-preserving consensus algorithm for integrated energy systems,” *IEEE Trans. Ind. Informat.*, early access, Oct. 29, 2024, doi: 10.1109/TII.2024.3475418.
- [8] J. A. Pinto, K. P. Vittal, and K. M. Sharma, “Passive islanding detection scheme based on instantaneous voltage and current for a multi-DG microgrid,” *IEEE Access*, vol. 12, pp. 160715–160727, 2024.
- [9] A. Hussain, C.-H. Kim, and M. S. Jabbar, “An intelligent deep convolutional neural networks-based islanding detection for multi-DG systems,” *IEEE Access*, vol. 10, pp. 131920–131931, 2022.
- [10] T. S. Tran, D. T. Nguyen, and G. Fujita, “Islanding detection method based on injecting perturbation signal and rate of change of output power in DC grid-connected photovoltaic system,” *Energies*, vol. 11, no. 5, p. 1313, May 2018.
- [11] D. Motter and J. C. M. Vieira, “Improving the islanding detection performance of passive protection by using the undervoltage block function,” *Electric Power Syst. Res.*, vol. 184, Jul. 2020, Art. no. 106293.
- [12] M. R. Alam, Most. T. A. Begum, and K. M. Muttaqi, “Assessing the performance of ROCOF relay for anti-islanding protection of distributed generation under subcritical region of power imbalance,” *IEEE Trans. Ind. Appl.*, vol. 55, no. 5, pp. 5395–5405, Sep. 2019.
- [13] W.-Y. Chang, “A hybrid islanding detection method for distributed synchronous generators,” in *Proc. Int. Power Electron. Conf.*, Jun. 2010, pp. 1326–1330.
- [14] S. Akhlaghi, M. Sarailoo, A. Akhlaghi, and A. A. Ghadimi, “A novel hybrid approach using sms and ROCOF for islanding detection of inverter-based DGs,” in *Proc. IEEE Power Energy Conf. Illinois (PECI)*, Feb. 2017, pp. 1–7.
- [15] H. R. Baghaee, D. Mlakic, S. Nikolovski, and T. Dragicccvic, “Anti-islanding protection of PV-based microgrids consisting of PHEVs using SVMs,” *IEEE Trans. Smart Grid*, vol. 11, no. 1, pp. 483–500, Jan. 2020.
- [16] S. K. G. Manikonda and D. N. Gaonkar, “IDM based on image classification with CNN,” *J. Eng.*, vol. 2019, no. 10, pp. 7256–7262, Oct. 2019.
- [17] A. A. Abdelsalam, A. A. Salem, E. S. Oda, and A. A. Eldesouky, “Islanding detection of microgrid incorporating inverter based DGs using long short-term memory network,” *IEEE Access*, vol. 8, pp. 106471–106486, 2020.
- [18] C. Wang, Z. Wang, S. Chu, H. Ma, N. Yang, Z. Zhao, C. S. Lai, and L. L. Lai, “A two-stage underfrequency load shedding strategy for microgrid groups considering risk avoidance,” *Appl. Energy*, vol. 367, Aug. 2024, Art. no. 123343.
- [19] C. Wang, Q. Dong, S. Mei, X. Li, S. Kang, and H. Wang, “Seamless transition control strategy for three/single-phase multimicrogrids during unintentional islanding scenarios,” *Int. J. Electr. Power Energy Syst.*, vol. 133, Dec. 2021, Art. no. 107257.
- [20] W. Li, S. Lin, H. Wu, and A. Zhang, “Islanding strategy based on dynamic programming algorithm for distribution network,” *Electric Power Autom. Equip.*, vol. 37, no. 1, pp. 47–52, Jan. 2017.
- [21] Z. N. Popovic, S. D. Knezevic, and B. S. Brbaklic, “A risk management procedure for island partitioning of automated radial distribution networks with distributed generators,” *IEEE Trans. Power Syst.*, vol. 35, no. 5, pp. 3895–3905, Sep. 2020.
- [22] J. Zhu, W. Gu, P. Jiang, Z. Wu, X. Yuan, and Y. Nie, “Integrated approach for optimal island partition and power dispatch,” *J. Modern Power Syst. Clean Energy*, vol. 6, no. 3, pp. 449–462, May 2018.
- [23] W. T. El-Sayed, H. E. Z. Farag, H. H. Zeineldin, and E. F. El-Saadany, “Formation of islanded droop-based microgrids with optimum loadability,” *IEEE Trans. Power Syst.*, vol. 37, no. 2, pp. 1564–1576, Mar. 2022.
- [24] Z. Hu, R. Guo, H. Lan, H. Liu, T. Sang, and F. Zhao, “Islanding model of distribution systems with distributed generators based on directed graph,” *Autom. Elect. Power Syst.*, vol. 39, no. 14, pp. 97–104, Jul. 2015.
- [25] X. Wang and J. Ling, “Island partition of the distribution system with distributed generation based on branch and bound algorithm,” *Proc. CSEE*, vol. 31, no. 7, pp. 16–20, Mar. 2011.
- [26] Z. Li, T. Khrebtova, N. Zhao, Z. Zhang, and Y. Fu, “Bi-level service restoration strategy for active distribution system considering different types of energy supply sources,” *IET Gener., Transmiss. Distribution*, vol. 14, no. 19, pp. 4186–4194, Oct. 2020.
- [27] Z. Yang, Y. Xia, W. Hu, J. Jing, and L. Chen, “Dynamic island partition strategy for active distribution system with controllable load participation,” in *Proc. IEEE Sustain. Power Energy Conf. (ISPEC)*, Nov. 2020, pp. 1927–1932.
- [28] Y. Xiang, J. Liu, L. Yao, and Y. Liu, “Optimization strategy for island partitioning and reconfiguration of faulted distribution network containing distributed generation,” *Power Syst. Technol.*, vol. 37, no. 4, pp. 1025–1032, Apr. 2013.
- [29] H. Yu, H. Mei, and H. Cheng, “Fault restoration of distribution network considering island operation of distributed power generation,” *Water Resour. Power*, vol. 33, no. 11, pp. 192–196, Nov. 2015.

- [30] P. Chen, H. Cheng, J. Lv, and H. Zhang, "Fault recovery of active distribution network considering active management based on second-order cone programming," *Electr. Meas. Instrum.*, vol. 56, no. 21, pp. 124–128, Nov. 2019.
- [31] X. Xie, F. Wang, Q. Chen, and C. Chen, "A method to ensure power supply reliability for key load in distribution network containing distributed generation," *Power Syst. Technol.*, vol. 37, no. 5, pp. 1447–1453, May 2013.
- [32] W. Lin, J. Zhu, Y. Yuan, and H. Wu, "Robust optimization for island partition of distribution system considering load forecasting error," *IEEE Access*, vol. 7, pp. 64247–64255, 2019.
- [33] Q. Li, S. Dai, X. Li, W. Li, and W. Sun, "Graph convolution networks-based island partition for energy and information coupled active distribution systems," in *Proc. IEEE Int. Conf. Commun., Control, Comput. Technol. Smart Grids (SmartGridComm)*, Oct. 2021, pp. 315–320.
- [34] C. Wang, S. Chu, Y. Ying, A. Wang, R. Chen, H. Xu, and B. Zhu, "Underfrequency load shedding scheme for islanded microgrids considering objective and subjective weight of loads," *IEEE Trans. Smart Grid*, vol. 14, no. 2, pp. 899–913, Mar. 2023.
- [35] J. Dou, H. Ma, J. Yang, Y. Zhang, and R. Guo, "An improved power quality evaluation for LED lamp based on G1-entropy method," *IEEE Access*, vol. 9, pp. 111171–111180, 2021.
- [36] M. E. Arce, Á. Saavedra, J. L. Míguez, and E. Granada, "The use of grey-based methods in multi-criteria decision analysis for the evaluation of sustainable energy systems: A review," *Renew. Sustain. Energy Rev.*, vol. 47, pp. 924–932, Jul. 2015.
- [37] Y. Jiang, C. Xu, Y. Liu, and K. Zhao, "A new approach for representing and processing uncertainty knowledge," in *Proc. 5th IEEE Workshop Mobile Comput. Syst. Appl.*, Las Vegas, NV, USA, Oct. 2003, pp. 466–470.
- [38] Y. Li and R. Huang, "A comprehensive review of set pair analysis," *IEEE Trans. Syst.*, vol. 46, no. 5, pp. 637–646, May 2017.
- [39] M. Yang, L. Zhang, Y. Cui, Y. Zhou, Y. Chen, and G. Yan, "Investigating the wind power smoothing effect using set pair analysis," *IEEE Trans. Sustain. Energy*, vol. 11, no. 3, pp. 1161–1172, Jul. 2020.
- [40] T. Wang, J.-S. Chen, T. Wang, and S. Wang, "Entropy weight-set pair analysis based on tracer techniques for dam leakage investigation," *Natural Hazards*, vol. 76, no. 2, pp. 747–767, Mar. 2015.
- [41] X. Dong and Y. Lu, "Islanding algorithm for distributed generators based on improved prim algorithm," *Power Syst. Technol.*, vol. 34, no. 9, pp. 195–201, Sep. 2010.
- [42] M. Davari, W. Gao, Z.-P. Jiang, and F. L. Lewis, "An optimal primary frequency control based on adaptive dynamic programming for islanded modernized microgrids," *IEEE Trans. Autom. Sci. Eng.*, vol. 18, no. 3, pp. 1109–1121, Jul. 2021.



LI ZHOU is currently a Senior Engineer with the State Grid Hubei Economic Research Institute. His current research interests include operation optimization of smart grids and microgrid analysis and microgrid control.



ZHIWEI LI is currently a Senior Engineer with the State Grid Hubei Economic Research Institute. His current research interests include power system analysis and microgrid operation and control.



WEI WANG is currently an Engineer with the State Grid Hubei Economic Research Institute. His current research interests include active distribution networks and microgrid control.



ZHAOYANG ZHANG is currently a Senior Engineer with the State Grid Hubei Economic Research Institute. His current research interests include microgrid operation and coordinated control and distributed generation.



SIHU CHU is currently with Hunan Electric Power Design Institute. His research interests include distributed power generation and microgrid system optimization.



HONG ZHANG is currently a Senior Engineer with the State Grid Hubei Economic Research Institute. His current research interests include microgrid energy management and integration of renewable energy sources.



WENHANG CHANG was born in Henan, China. She is currently pursuing the M.S. degree in electrical engineering with China Three Gorges University, Yichang, China. Her research interests include renewable energy systems and microgrid protocol control.



CAN WANG (Member, IEEE) was born in Hubei, China. He received the Ph.D. degree in electrical engineering from the South China University of Technology, Guangzhou, China, in 2017.

He is currently an Associate Professor in electrical engineering with the College of Electrical Engineering and New Energy, China Three Gorges University, Yichang, China. His current research interests include distributed generation, microgrid operation and control, integrated energy systems, and smart grids. He serves as the Co-Chair for the Special Session on “Power Systems with Penetration of RE and EV” in IEEE IGBSG 2019. He is a Young Editorial Board Member of the *Journal of China Electric Power*, *Electrical Construction and Maintenance*, and *Journal of Electric Power Science and Technology*. He is an Active Reviewer of IEEE TRANSACTIONS ON SUSTAINABLE ENERGY, IEEE TRANSACTIONS ON INDUSTRIAL ELECTRONICS, IEEE SYSTEMS JOURNAL, *IET Power Electronics*, *IET Renewable Power Generation*, and IEEE ACCESS.



ZHUOLI ZHAO (Senior Member, IEEE) received the Ph.D. degree in electrical engineering from the South China University of Technology, Guangzhou, China, in 2017. From 2014 to 2015, he was a Joint Ph.D. Student and a Sponsored Researcher with the Control and Power Research Group, Department of Electrical and Electronic Engineering, Imperial College London, London, U.K. From 2017 to 2018, he was a Research Associate with the Smart Grid Research Laboratory,

Electric Power Research Institute, China Southern Power Grid, Guangzhou, China. He is currently an Associate Professor with the School of Automation, Guangdong University of Technology, Guangzhou. His research interests include microgrid control and energy management, renewable power generation control, and smart grids.



CHUN SING LAI (Senior Member, IEEE) received the B.Eng. (Hons.) in electrical and electronic engineering from Brunel University London, London, U.K., in 2013, and the D.Phil. degree in engineering science from the University of Oxford, Oxford, U.K., in 2019. He is currently with the Department of Electronic and Electrical Engineering, Brunel University London, and also with the Department of Electrical Engineering, School of Automation, Guangdong University of

Technology. His major research interests include power dispatching automation of new energy sources, power system optimization, energy system modeling, operation and control of microgrid, and active distribution networks.



LOI LEI LAI (Life Fellow, IEEE) received the B.Sc. degree (Hons.) in electrical and electronic engineering from the University of Aston, Birmingham, U.K., in 1980, and the Ph.D. and D.Sc. degrees in electrical and electronic engineering from the City, University of London, London, U.K., in 1984 and 2005, respectively. He is currently an University Distinguished Professor with Guangdong University of Technology, Guangzhou, China. He was a Pao Yue Kong Chair

Professor with Zhejiang University, Hangzhou, China, and a Professor and the Chair in electrical engineering with the City, University of London. His major research interests include power system under high penetration of renewables, smart energy networks, operation and control of microgrid, and active distribution networks.

...